

# PCCP

Accepted Manuscript



This is an *Accepted Manuscript*, which has been through the Royal Society of Chemistry peer review process and has been accepted for publication.

*Accepted Manuscripts* are published online shortly after acceptance, before technical editing, formatting and proof reading. Using this free service, authors can make their results available to the community, in citable form, before we publish the edited article. We will replace this *Accepted Manuscript* with the edited and formatted *Advance Article* as soon as it is available.

You can find more information about *Accepted Manuscripts* in the [Information for Authors](#).

Please note that technical editing may introduce minor changes to the text and/or graphics, which may alter content. The journal's standard [Terms & Conditions](#) and the [Ethical guidelines](#) still apply. In no event shall the Royal Society of Chemistry be held responsible for any errors or omissions in this *Accepted Manuscript* or any consequences arising from the use of any information it contains.

# Enriching Physisorption of $H_2S$ and $NH_3$ Gases on a Graphane Sheet by doping with $Li$ adatoms

\*<sup>a</sup>Tanveer Hussain, \*<sup>a</sup> Puspamitra Panigrahi, and <sup>ab</sup> Rajeev Ahuja

We have used Density functional theory to investigate the adsorption efficiency of a hydrogenated graphene (graphane) sheet for  $H_2S$  and  $NH_3$  gases. We find neither the pristine graphane sheet nor the sheet defected by removing few surface  $H$  atoms have sufficient affinity for either  $H_2S$  or  $NH_3$  gas molecules. However, the graphane sheet doped with  $Li$  adatoms shows a strong sensing affinity for both the mentioned gas molecules. We have calculated the absorption energies with one [referred as half coverage] molecule and two molecules [referred as full coverage] for both the gases with the  $Li$ -doped graphane sheet. We find, for both the gases the calculated absorption energies are adequate enough to decide the  $Li$ -doped graphane sheet to be suitable for sensing  $H_2S$  and  $NH_3$  gases. The  $Li$ -doped sheet shows a higher affinity for the  $NH_3$  gas compared to  $H_2S$  gas molecules due to a stronger  $Li(s)$ - $N(p)$  hybridization compared to that of  $Li(s)$ - $S(p)$ . However, while going from half coverage effect to full coverage effect the calculated binding energies show a decreasing trend for both the gases. The calculated work function of the  $Li$ -doped graphane sheet decreases while bringing the gas molecules to its vicinity which explains the affinity of the sheet towards both the molecules.

## 1 Introduction

Graphene is the experimental isolation of a single atomic layer of carbon atoms arranged in a honeycomb lattice structure, forming the thinnest free standing material to date. The Dirac charge carriers in graphene and its large surface to volume ratio increases the probability of the chemical reaction of the surface atoms with various adsorbates. When an adsorbate (donors or acceptors) is exposed to the graphene surface, it changes the charge concentration and ultimately alters the electrical properties of the graphene surface; thus, opens the possibility for graphene as a future gas sensor<sup>1</sup>. In recent years, there have been a handful studies reporting the adsorption of selected gas molecules like  $CO$ ,  $NO$ ,  $NO_2$ ,  $N_2$ ,  $CO_2$ ,  $H_2O$ ,  $CO$ ,  $NO$  and  $NH_3$  on various graphene structures<sup>2,3</sup>, which predict graphene as an efficient sensor, having the potential to replace the conventional solid-state sensors<sup>2,3</sup>.

The introduction of heteroatoms to an ideal graphene sheet, entirely composed of  $C$  atoms, further changes its electronic as well as electrochemical properties to bring a tweak in its sensing aptitude. Recently, Ying *et al.* have reported the change in the electron density of the graphene sheet during nitrogen doping, which makes it an excellent candidate for glucose biosensing<sup>4</sup>.

However, compared to the heteroatomic substitution, a complete hydrogenation of graphene rather results in a graphane sheet( $CH$ )<sup>5,6</sup> which looks like a graphene painted

with hydrogen on both sides. The resulting graphane sheet retains the thinness, strength and flexibility but has a very different electronic properties from that of the parent graphene. The  $C-H$  bonding ties down the electrons which leads to an insulating behavior for graphane<sup>7</sup> and makes it an activated precursor for suitable chemical modifications<sup>8</sup>. Besides the robust transport properties, a comparatively larger adsorption energies with different adsorbates and the tunable band gap properties expose graphane as a superior candidate for the future gas sensing purposes<sup>9-14</sup>.

Though the carbon based nano structures like graphene, and graphane show a very little interaction with the adsorbents, a drastic improvement in the binding energies of some of the gas molecules, while introducing defects and dopants to the surface of pristine graphene and graphane structures, have already been reported elsewhere<sup>15-18</sup>. In particular, various alkali metals are reported to adhere to the graphene sheet without destroying its basic electronic properties while creating a surface charge redistribution and further changing the work function of the sheets<sup>19-22</sup>. In this context, a stable structure of the lithium-doped graphane( $CHLi$ ) sheet has already been reported and is found to be a prospective candidate for the future hydrogen storage<sup>23-25</sup>.

However, very few theoretical calculations so far have been reported on modulated graphane sheet, predicting its properties as an efficient gas sensor.

Among many,  $H_2S$  is one of the toxic gases which is extremely harmful for the human beings as well as for the atmosphere and it is found to be fatal if the concentration goes beyond 250 ppm<sup>26</sup>. Therefore, the detection, sensing and monitoring of  $H_2S$  gas at different circumstances is very important for us and our environment. On the other way, though  $NH_3$

<sup>a</sup>Condensed Matter Theory Group, Department of Physics and Astronomy, Box 516, Uppsala University S-75120 Uppsala, Sweden.

<sup>b</sup>Department of Materials and Engineering, Royal Institute of Technology (KTH) S-100 44 Stockholm, Sweden.

\* Corresponding author

gas is useful in various fields like in agriculture, industry, and medical, is rather considered as a toxic gas too when used at high concentration<sup>27</sup>. Thus, it is very much necessary to have an efficient sensor to avoid the dangerous consequences of the presence of such  $NH_3$  and  $H_2S$  gases when needed.

In this work, by using Density functional theory we have studied a defected graphane sheet ( $CH$ ) by introducing Hydrogen vacancies. We find, the absorption energies of the hydrogen deficient graphane sheet with  $NH_3$  and  $H_2S$  gases are not adequate enough for the sensing purpose. Further, we have doped the graphane sheet with two  $Li$  atoms at the Hydrogen sites. The  $Li$  atoms are kept far apart to avoid the clustering effect. We find a stable structure for this  $Li$ -doped graphane structure ( $CHLi$ ) which is having an ample amount of absorption energy for sensing  $NH_3$  and  $H_2S$  gases. We have calculated the absorption energies with one molecule and two molecules of both the gases with  $CHLi$  sheet. During this physisorption process the band gap of the  $CHLi$  structure shows a decreasing trend. However, while going from one molecules to two molecules the absorption energies show an decreasing trend for both the gases.

## 2 Computational Methods

We have performed first principles DFT calculations using projector augmented wave method (PAW) as implemented within VASP package<sup>28–31</sup>. The approximation to the exchange and correlation potential is executed using Perdew-Burke-Ernzerhof functional<sup>32</sup>. The graphane ( $CH$ ) sheet is modeled as a  $4 \times 4 \times 1$  supercell having 64 atoms ( $C_{32}H_{32}$ ) for this study. In order to have a  $Li$ -doped graphane sheet ( $C_{32}H_{30}Li_2$ ), the two  $Li$  atoms are substituted at the  $H$  site as shown in Fig. 1(a,b). During the periodic calculation a vacuum space of  $15 \text{ \AA}$  has been inserted along the  $z$  direction to minimize the interaction between the periodic images of the mentioned sheets.

To investigate the sensing mechanism of  $H_2S$  and  $NH_3$  on the  $Li$ -doped graphane sheet we have exposed the  $C_{32}H_{30}Li_2$  sheet first with one formula unit of  $H_2S$  and  $NH_3$  molecules separately as shown in Fig 2 (a, b) and Fig 3 (a, b) respectively. In the next step we have introduced the  $Li$ -doped graphane sheet with two formula unit of  $H_2S$  and  $NH_3$  molecules in the similar fashion as shown in Fig 2 (c, d) and Fig 3 (c, d).

For sampling the Brillouin zone, we have used a dense ( $5 \times 5 \times 3$ )  $k$ -points mesh in Monkhorst-Pack<sup>33</sup> schemes. For

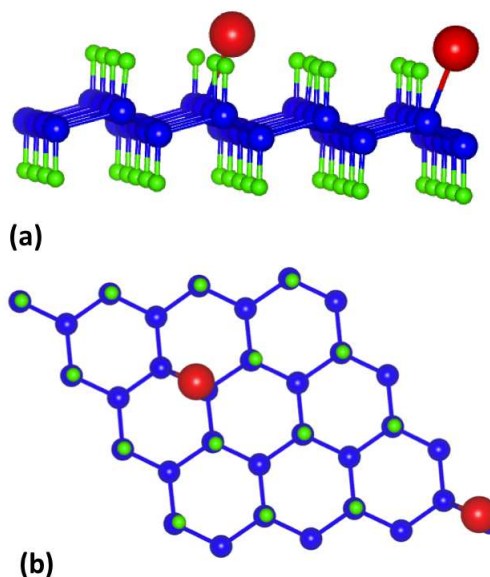


**Fig. 1** (color on line) Side view (a) and top view (b) of the optimized structure of  $C_{32}H_{30}Li_2$  sheet, blue, green and red balls represent C, H and Li atoms respectively.

getting ground state of all the above mentioned structures, we have kept the criterion of forces acting on each ion to be less than  $0.005 \text{ eV/\AA}$ . A very accurate converged energy cut off of  $450 \text{ eV}$  have been used for the plane wave basis set. In our conventional DFT calculation, the approximation of exchange correlation potential within Local density approximation (LDA) overestimates the binding energies but performs better job in case of weakly interacting systems whereas the generalized gradient approximation (GGA) usually underestimates the binding energies. To have a better description of  $H_2S$  and  $NH_3$  physisorption over  $CHLi$ , we have used LDA approximations along with the van der Waals correction as implemented in the DFT-D2 approach by Grimme<sup>34</sup> within the VASP package and benchmarked by Tomas *et al*<sup>35</sup>. Here, a semi-empirical dispersion potential is added to our conventional Kohn-Sham DFT energy.

To have a better understanding of adsorption effect of  $H_2S$  and  $NH_3$  on defected  $C_{32}H_{30}Li_2$  graphane sheet, we have calculated the work function  $\phi$  of the bare and physisorbed sheets as;

$$\phi = V(\phi) - E_f \quad (1)$$

Where,  $\phi$ ,  $V(\phi)$  and  $E_f$  are the work function, electrostatic potential at vacuum level and the Fermi energy of the  $Li$ -doped graphane sheet respectively.

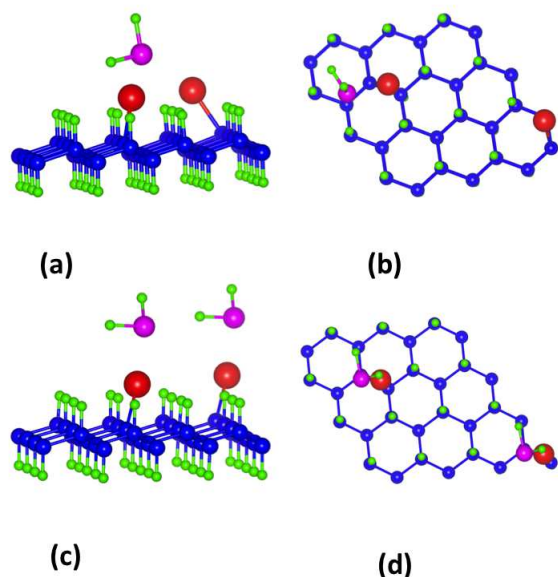


**Fig. 2** (color on line) Side view (a,c) and top (b,d) of the optimized structure of  $C_{32}H_{30}Li_2$  sheet physisorbed with  $H_2S$  gas molecule, Blue, green, red and magenta balls represent C, H, Li and S atoms respectively. Here Fig (a, b) are for half coverage and (c,d) presents full coverage effect respectively.

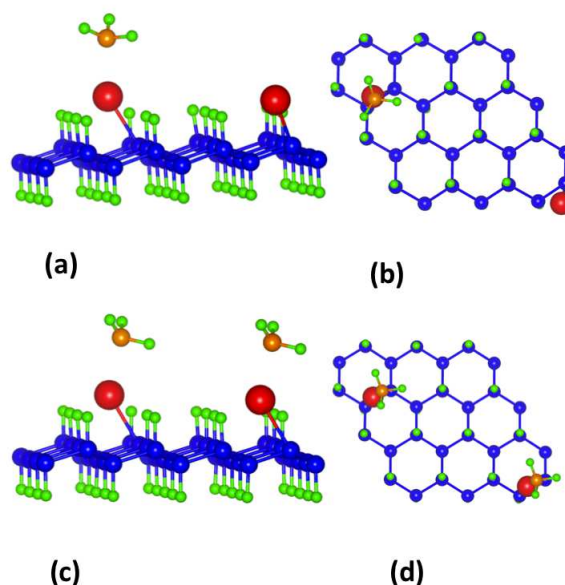


**Fig. 3** (color on line) Side view (a,c) and top (b,d) of the optimized structure of  $C_{32}H_{30}Li_2$  sheet physisorbed with  $NH_3$  gas molecule, Blue, green, red and orange balls represent C, H, Li and N atoms respectively. Here Fig (a, b) are for half coverage and (c,d) presents full coverage effect respectively.

### 3 Results and Discussion

Here onwards, we have divided our results in three different parts. In the first part we have discussed the structural properties of the *Li*-doped graphane sheet. In the second part we have considered the absorption mechanism of  $H_2S$  on graphane sheet at different concentrations and the third part deals with that of  $NH_3$  on graphane sheet.

#### 3.1 Structural properties of *Li*-doped graphane

A complete hydrogenation turns the metallic graphene to a wide band gap ( $\sim 5$  eV) graphane (CH). Our optimized structure of the 64 atom pristine graphane sheet doped with *Li* as a  $C_{32}H_{30}Li_2$  graphane sheet is shown in the Figure 1(a, b). In the *Li*-doped optimized graphane sheet the  $C-C$ ,  $C-H$  and  $C-Li$  bond lengths are found to be  $1.54$  Å,  $1.10$  Å and  $1.98$  Å respectively.

However, for an efficient utilization of a metal functionalized graphane sheet, the metal to graphane binding should be always high enough to prevent the metal-metal clustering effect which could cease the performance of a designed sensor. Thus, it is important to maintain a reasonably high adatom-adatom distance (low doping concentration) on the defected

graphane sheet to avoid the clustering effect<sup>25</sup>. Here, in the modeled *Li* doped graphane sheet, we have maintained a distance of  $8.8$  Å between the two *Li* adatoms. The binding energy is estimated to be  $-2.3$  eV per *Li* atom. A significant decreasing trend in the binding energies of the *Li* doped graphane sheet while increasing the *Li* doping concentration from 50% to 3.12% has already been reported in previous studies<sup>36,37</sup>. At higher doping concentration, the possibility of clustering between the *Li* adatoms ultimately lowers the binding energies of the *Li* doped graphane sheet; thus a 3.12% of *Li* doping concentration is carefully maintained for this current study. The band gap of the defected  $C_{32}H_{30}$  graphane sheet (two *H* atoms are removed) is calculated to be  $\sim 1.5$  eV and when doped with *Li*, the band gap of the  $C_{32}H_{30}Li_2$  graphane sheet further reduces 0.96 eV (Table 1) which is also evident from the density of states (DOS) plot as shown in Fig. 4 (a,b). Very similar metallic behavior for the graphane sheet, having higher doping concentration of different metal adatoms like *Li*, *Na*, *K*, *Be*, *Mg*, and *Ca*, have also been reported else where<sup>18,20,25</sup>. Other than that, compared to other adatoms, the *Li* to graphane sheet binding energy is found to be higher. The strong CH-*Li* binding allows the uniform distribution of *Li* over the sheet and also nullifies the possibility of *Li*-*Li* cluster formation, which is highly desirable to preserve the reversibil-

ity of the designed system.

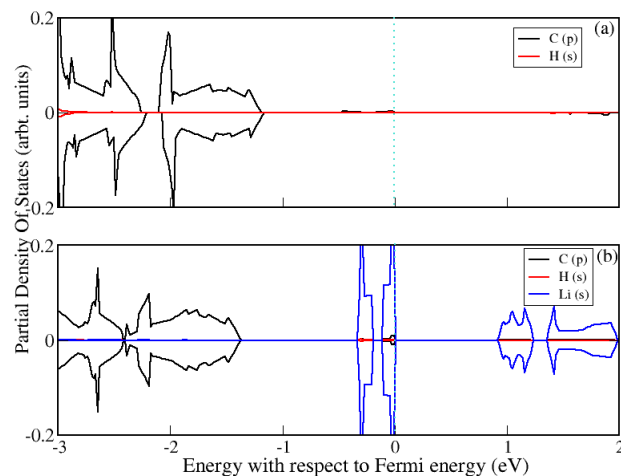


**Fig. 4** (color on line) Fig (a) is the Partial DOS plot of  $C(p)$ , and  $H(s)$  of defected graphane sheet. Fig (b) is that of the  $C(p)$ ,  $H(s)$ , and  $Li(s)$  in the  $C_{32}H_{30}Li_2$  sheet.

From the DOS plot we see the valence band regions near the Fermi energy is mostly dominated by  $Li(s)$ ; the band gap of the defected  $C_{32}H_{30}$  graphane sheet got reduced while introducing  $Li$  to the sheet. Near the Fermi energy we find a  $C(p) - Li(s)$  hybridization which leads to an increase in binding energy per  $Li$  atom for the doped  $C_{32}H_{30}Li_2$  sheet by 2.5 eV. Henceforth, the graphane sheet doped with  $Li$  which results in gain in binding energy leads to a comparatively stabler  $C_{32}H_{30}Li_2$  graphane sheet and will be further discussed for the sensing of  $H_2S$  and  $NH_3$  gases.

### 3.2 Adsorption Energy of $H_2S$

Our rigorous computation leads to the most preferred structure for the  $H_2S$  molecule over the  $C_{32}H_{30}Li_2$  sheet as shown in Fig 2 (a,b) (c, d) for one [refereed as half coverage] and two  $H_2S$  molecules [refereed as full coverage] respectively. We have calculated the adsorption energies as well as the band gap of the resulting structures in terms of coverage effect. The average distance of the  $H_2S$  molecule from the  $C_{32}H_{30}Li_2$  sheet is found to be same 2.47 Å for both the coverage effect. With the half coverage effect, the estimated binding is -0.44 eV and that with full coverage effect turns out to be -0.36 eV. The negative sign indicates the affinity of  $Li$ -doped graphene sheet towards the  $H_2S$  molecule. Thus, with increase in coverage effect the affinity shows a decreasing trend. On the other hand, the estimated binding energies of  $H_2S$  molecule on defected graphane sheet  $C_{32}H_{30}$  without  $Li$  doping are found to be with +ve sign

which shows that affinity of defected graphane sheet towards  $H_2S$  is inadequate enough to solve the purpose of a gas sensor. To get confidence about our results, we have performed all the calculation using LDA approach as well as van der Waals correction approach as implemented in the DFT-D2. Here, the binding energies of  $C_{32}H_{30}Li_2$  sheet physisorbed with  $H_2S$  estimated from both the methods are summarized in Table 1. We have found a similar decreasing trend in the adsorption energy with half coverage effect to full coverage effect in both the methods (Table 1). The estimated band gap also shows a decreasing trend from 1.1 eV to 0.67 eV while going from half to full coverage effect (Table 1). To understand the electronic structure of the physisorbed system we have plotted the partial density of states (PDOS) of  $C(p)$ ,  $Li(s)$ ,  $S(p)$  and  $H(s)$  as shown in Fig 5 (a). We find, the  $S(p)$  shows a strong hybridization with  $C(p)$  as well as with  $Li(s)$  near the Fermi energy [Fig 5(a)] which explains the affinity of  $Li$ -doped graphane sheet towards  $H_2S$  gas molecule. However, with full coverage effect  $Li(s)$  bands gets broadened near the fermi energy compared to the half coverage effect. With increasing  $S$  concentration the extra  $S(p)$  bands are rather more spreaded to the conduction band region which are not participating strongly to the parent  $C_{32}H_{30}Li_2$  sheet. Thus, the affinity decreases with increasing the concentration of gas molecule.

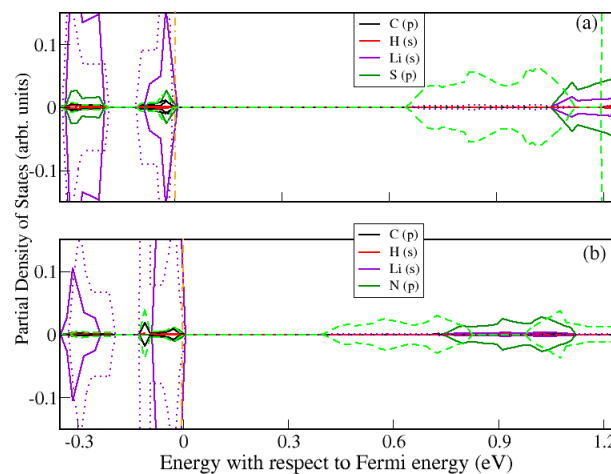


**Fig. 5** (color on line) Fig (a) is the Partial DOS plot of  $C(p)$ ,  $H(s)$ ,  $Li(s)$  and  $S(p)$  of the  $C_{32}H_{30}Li_2$  sheet physisorbed with  $H_2S$  gas molecule whereas Fig (b) shows that of the  $C(p)$ ,  $H(s)$ ,  $Li(s)$  and  $N(p)$  of the  $C_{32}H_{30}Li_2$  sheet physisorbed with  $NH_3$  gas. The solid line presents the half coverage effect whereas the dotted line shows the full coverage effect for both the gases.

**Table 1** The adsorption energies  $E_{ads}$  in eV calculated with LDA and van der Waals (Vdw) approaches. CHLi represents the Li-doped graphane sheet. CHLi –  $H_2S$  and CHLi –  $NH_3$  presents the CHLi sheet exposed to  $H_2S$  and  $NH_3$  gases.

System	Coverage	LDA- $E_{ads}$ (eV/molecule)	Vdw- $E_{ads}$ (eV/molecule)	band gap (eV)	workfunction( $\phi$ ) (eV)
CHLi	-	-	-	0.96	2.76
CHLi – $H_2S$	half	-0.92	-0.43	1.10	2.68
	full	-0.76	-0.36	0.67	2.42
CHLi – $NH_3$	half	-1.35	-0.83	0.76	2.44
	full	-1.10	-0.76	0.43	2.11

### 3.3 Adsorption Energy of $NH_3$

We have performed our calculation for  $NH_3$  gas over the the  $C_{32}H_{30}Li_2$  sheet in the similar fashion as that of  $H_2S$  molecule. The most preferred optimized configurations of  $NH_3$  over  $C_{32}H_{30}Li_2$  sheet with half coverage and full coverage are shown in Fig 3 (a, b) and (c, d) respectively. The average bond distance from  $NH_3$  to  $C_{32}H_{30}Li_2$  sheet is found to be  $\sim 2.03$  Å for both the coverage effect. However, unlike  $H_2S$  the  $NH_3$  molecule undergoes a structural relaxation in presence of  $C_{32}H_{30}Li_2$  sheet. The  $N-H$  bond distance which is  $1.017$  Å in its isolated configuration becomes  $1.023$  Å and  $1.025$  Å with half and full coverage effect respectively. Also the initial  $H-N-H$  bond angle changes from  $107.80^\circ$  to  $107.630^\circ$ . For  $NH_3$  gas molecule, the binding energies are estimated to be  $-0.83$  eV and  $-0.76$  eV per molecule for the half coverage and full coverage respectively which are higher compared to that of  $H_2S$ . The details of binding energy calculation with van der Waals correction are give in Table 1. Here, the band gap also shows a similar decreasing trend from  $0.76$  eV to  $0.43$  eV like the previous one (Table1). We have also plotted the partial density of states (PDOS) of  $C(p)$ ,  $Li(s)$ ,  $N(p)$  and  $H(s)$  as shown in Fig 5(b). We find, there is a strong hybridization between  $C(p)$  with  $N(p)$  here compared to that of  $C(p)$  with  $S(p)$  in the  $H_2S$  physisorbed graphane sheet [Fig 5(a)]. The  $C(p)$  and  $N(p)$  have also strong hybridization with  $Li(s)$  near the Fermi energy [Fig 5(b)]; which leads to higher affinity of Li-doped graphane sheet towards  $NH_3$  gas molecule compared to that for the  $H_2S$  gas molecule (Table 1). With full coverage effect of  $NH_3$ , similar decreasing effect is happening like that of  $H_2S$  gas molecule.

### 3.4 Change in Work Function ( $\phi$ )

The surface reactivity of the doped graphane sheet towards the gas molecule will mostly depend upon the surface potential variation which could be perceived by the change in work function  $\phi$ . The work function is the minimum amount of energy required to remove the electron from the Fermi level

to far enough. While the electron moves through the surface region, the  $\phi$  becomes sensitive towards any changes at the surface in presence of other gas molecules. Thus, the change in  $\phi$  could determine the operating condition of the Li-doped graphane sheet as a gas sensor. Since, during the physisorption process the gas molecules introduce a net dipole moment due to a charge transfer between the surface and the gas molecule. Thus, there will be a shift in work function which could further change the sensing properties of the system<sup>38-41</sup>. Here, we have calculated the work function as per equ. 1 for the bare  $C_{32}H_{30}Li_2$  sheet and while the sheet is physisorbed with  $H_2S$ , and  $NH_3$  at different coverage effect and summarized in Table1. We find both  $H_2S$ , and  $NH_3$  molecules shows a decreasing trend in the work function for the physisorbed sheet compared to the bare sheet and the resulting work functions even get smaller when we go from full coverage to half coverage effect (Table 1). In general, the  $\phi$  depends upon the the energy difference between the Fermi level and conduction band. We find from our PDOS plots as shown in Fig 5 (a,b), for both the gas molecules while going from half coverage effect to full coverage effect the energy difference between the Fermi level to the conduction band decreases so do the work functions (Table 1). From our Bader charge analysis<sup>42</sup> we find, in the case of pristine  $C_{32}H_{30}Li_2$  sheet, as mentioned before, two H atoms have been replaced with Li atoms. Due to higher electronegativity of C than Li, there is a charge transfer from Li to C. Our analysis reveals that  $0.98 e$  of charge have been transferred from both Li adatoms and accumulated at the C sites which are bonded directly with Li atoms. However, a small fraction of these charge will be acquired by those H atoms laying in the vicinity of C and Li atoms which leads to a state where the Li are with partial positive charge. In case of  $H_2S$  adsorption for both the coverage effect, there is hardly any transfer of charge from  $H_2S$  to the  $C_{32}H_{30}Li_2$  sheet. There is interchange of electric charge within the  $H_2S$  molecules and the interaction of incident molecules with the sheet is due to weak van der Waals type of interaction. Whereas in case of  $NH_3$  molecules the H atoms transfer their charge to the N

atom within the molecule resulting into a net negative charge on  $N$  and positive charge on  $H$  atoms. During exposure of  $NH_3$  molecules to the  $C_{32}H_{30}Li_2$  sheet, precisely 0.06  $e$  and 0.01  $e$  unit of charge have been transferred to  $N$  atoms from  $Li$  atoms in case of half and full coverage effect respectively.

#### 4 Summary

In summary, the absorption of  $H_2S$  and  $NH_3$  gas molecules on  $Li$ -doped graphane sheet is investigated by using Density functional theory. We find both the molecules are very well physisorbed onto the  $Li$ -doped graphane sheet. However, the sheet has a higher affinity for the  $NH_3$  gas molecule compared to  $H_2S$  gas molecule. The  $C(p)$ - $N(p)$  hybridization in case of  $NH_3$  physisorption is more efficient compared to that of  $C(p)$ - $S(p)$  hybridization during  $H_2S$  physisorption. However, while increasing the concentration of both the gases while exposing to the graphane sheet, the affinity shows a decreasing trend. The work function ( $\phi$ ) which determines the surface reactivity also shows a decreasing trend for the  $Li$ -doped graphane sheet during physisorption of both the gas molecules. A very similar trend is observed for the calculated binding energies while using the LDA potential as well as with the van der Waals correction as implemented in the DFT-D2 approach which gives the confidence for the robustness of our approach.

#### 5 acknowledgement

Thanveer Hussien is thankful to the higher education commission of Pakistan for his doctoral fellowship. Puspamitra Panigrahi is grateful to the Swedish Institute for her postdoctoral Fellowship. SNIC and UPPMAX are acknowledged for providing computing resources.

#### References

- 1 F. Schedin, A. K Geim, S. V. Morozov, E. W. Hill, P. Blake, M. I. Katsnelson, K. S. Novoselov, Nature Mat. 2007, **6**, 652.
- 2 B. Huang, Z. Li, Z. Liu, G. Zhou, S. Hao, J. Wu, B. -L. Gu, W. H. Duan, J. Phys. Chem. C 2008, **112**, 13442.
- 3 O. Leenaerts, B. Partoens, F. M. Peeters, Phys. Rev. B 2008, **77**, 125416.
- 4 Y. Wang, Y. Shao, D. W. Matson, J. Li and Y. Lin, ACS Nano, 2010, **4**, 1790.
- 5 J. O. Sofo, A. S Chaudhari, G. D. Barber, Phys. Rev. B 2007, **75**, 153401.
- 6 D. C. Elias, R. R Nair, T. M. G Mohiuddin, S. V Morozov, P Blake, M. P. Halsall, A. C Ferrari, D. W Boukhvalov, A.K. Geim, K. Novoselov, Science 2009, **323**, 610.
- 7 S. Lebegue, M. Klintonberg, O. Eriksson, M.I. Katsnelson, Phys. Rev. B 2009, **79**, 245117.
- 8 Z. Sun, C. L. Pint, D. C. Marcano, C. Zhang, J. Yao, G. Ruan, Z. Yan, Y. Zhu, R. H. Hauge and J. M. Tour, Nat. Commun., 2011, **2**, 559.
- 9 C. K. Yang, Appl. Phys. Lett. 2009, **94**, 163115.
- 10 H. Sahin, C. Ataca, S. Ciraci, Phys. Rev. B 2010, **81**, 205417.
- 11 J. Berashevich, T. Chakraborty, Phys. Rev. B 2010, **82**, 134415.
- 12 L. F. Huang, X. H. Zheng, G. R. Zhang, L. Li, Z. J. Zeng, J. Phys. Chem. C 2011, **115**, 21088.
- 13 T. Hussain, B. Pathak, M. Ramzan, T. A Maark, R. Ahuja, Appl. Phys. Lett. 2012, **100**, 183902.
- 14 M. Nava, D. E. Galli, M.W Cole, L. Reatto, Phys. Rev. B 2012, **86**, 174509.
- 15 Y-H. Zhang, Y-B Chen, K-G Zhou, C-H Liu, J. Zeng, H. L Zhang, Y. Peng, Nanotechnology 2009, **20**, 185504.
- 16 M. Gautam, A. H. Jayatissa, J. Appl. Phys. 2012, **112**, 114326.
- 17 H. Sahin, C. Ataca, S. Ciraci, Appl. Phys. Lett. 2009, **95**, 222510.
- 18 T. Hussain, B. Pathak, T. A Maark, M. Ramzan, R. Ahuja, Euro Phys. Lett. 2012, **99**, 47004.
- 19 A. Politano, G. Chiarello, J. Chem. Phys. 2013 **138**, 044703.
- 20 P. Medeiros, F. Mota, A. Mascarenhas, C. Castilho, Nanotechnology, 2010 **21**, 115701.
- 21 D. Boukhvalov, C. Virojanadara, Nanoscale 2012, **4**, 1749.
- 22 K. Jin, S. Choi, S. Jhi, Phys. Rev. B 2010, **82**, 033414.
- 23 M. Khanzai, M. S Bahramy, N. S Venkataramanan, H. Mizuseki, Y. Kawazoe, J. Appl. Phys. 2009, **106**, 094303.
- 24 T. Hussain, A. D Sarkar, R. Ahuja, Appl. Phys. Lett. 2012, **101**, 103907.
- 25 L. Antipina, P. Avramov, S. Sakai, H. Naramoto, M. Ohtomo, S. Entani, Y. Matsumoto, P. Sorokin, Phys. Rev. B 2012, **86**, 085435.
- 26 W. H. Tao, C. H. Tsai, Sens. Actuators B 2002, **81**, 237.
- 27 Z. Wu, X. Chen, S. Zhu, Z. Zhou, Y. Yao, W. Quan, B. Liu, Sens. Actuators B 2013, **178**, 485.
- 28 P. E Blochl, Phys. Rev. B 1994, **50**, 17953.
- 29 G. Kresse, J. Hafner, Phys. Rev. B 1993, **47**, 558.
- 30 G. Kresse, J. Hafner, Phys. Rev. B 1994, **49**, 14251.
- 31 G. Kresse, D. Joubert, Phys. Rev. B 1999, **59**, 1758.
- 32 J. P. Perdew, J. A. Chevary, S. H. Vosko, K. A Jackson, M. R. Pederson, D. J. Singh, C. Fiolhais, Phys. Rev. B 1992, **46**, 6671.
- 33 H. J. Monkhorst, J. D. Pack, Phys. Rev. B 1976, **13**, 5188.
- 34 J. J. Grimme, Comput. Chem. 2006, **27**, 1787.

- 
- 35 T. Bucko, J. Hafner, S. Lebegue, J.G. Angyan, *J. Phys. Chem. A* 2010, **114**, 11814.
  - 36 T. Hussain, B. Pathak, T. A. Maark, M. Ramzan, R. Ahuja, *Euro. Phys. Lett* 2012, **99**, 47004.
  - 37 T. Hussain, B. Pathak, T. A. Maark, C. Moyses, R. Scheicher, Rajeev Ahuja, *Euro. Phys. Lett* 2011, **96**, 27013.
  - 38 Y. Paska, T. Stelzner, S. Christiansen, H. Haick, *ACS Nano* 2011, **5**, 5620.
  - 39 G. Heimel, L. Romaner, J. Bredas, E. Zojer, *Phys. Rev. Lett.* 2006, **96**, 196806.
  - 40 A. Natan, L. Kronik, H. Haick, R. Tung, *Adv. Mater.* 2007, **19**, 4103.
  - 41 N. Barsan, D. Koziej, U. Weimar, *Sens. Actuators B* 2007, **121**, 18235.
  - 42 G. Henkelman, A. Arnaldsson, and H. Jansson, *Comput. Mater. Sci.* 2006, **36**, 254.